Trogocytosis-mediated transfer of FOLR2 from Nurse-like cells to CLL cells is linked to their activation and proliferation

Marcin Domagala[1], Bastien Gerby[1], Chloe Bazile[1], Loïc Ysebaert[1,3], Vera Pancaldi[1], Camille Laurent[1,2] and Mary Poupot [1*]

[1] CRCT, UMR1037 Inserm-Univ. Toulouse III Paul Sabatier-ERL5294 CNRS, 2 avenue Hubert Curien Oncopole de Toulouse, CS53717, 31037, Toulouse, France.
[2] Service d'anatomopathologie, Institut Universitaire du Cancer de Toulouse - Oncopôle, 31059 Toulouse, France.
[3] Department of Haematology, Institut Universitaire du Cancer de Toulouse - Oncopôle, 31059 Toulouse, France.

Corresponding authors: Marcin Domagala (marcin.domagala@inserm.fr) and Mary Poupot (mary.poupot@inserm.fr); 2 avenue Hubert Curien Oncopole de Toulouse, CS53717, 31037, Toulouse, France. phone: +335 82 74 16 62, fax: +335 82 74 16 85.

KEY POINTS

- FOLR2 is a marker of M2-like protective NLCs
- CLL cells acquire functional FOLR2 from NLCs through trogocytosis, enabling them to enhance folate uptake
- Trogocytic FOLR2$^+$ CLL cells are enriched in the fraction of activated and proliferative cells, especially during folic acid scarcity
- Detection of FOLR2$^+$ NLCs and FOLR2$^+$ trogocytic CLL cells in the LNs of CLL patients.

ABSTRACT

This study, conducted on primary human samples, identifies a novel pro-tumoral interaction between nurse-like cells (NLCs) and chronic lymphocytic leukemia (CLL) cells, relying on the trogocytosis-mediated transfer of functional Folate Receptor β (FOLR2) from NLCs to cancer cells. Trogocytic CLL cells carrying NLC-derived FOLR2 exhibit an enhanced capacity for folic acid internalization. Furthermore, induction of the proliferative state of CLL cells with CD40L+IL-15 treatment in the presence of NLCs, to imitate lymph node (LN) environment *in vitro*, revealed that trogocytic FOLR2$^+$ cancer cells are enriched in the fraction of active and proliferating cells, particularly under condition of folic acid depletion. FOLR2 remains detectable on CLL cells as long as they maintain their proliferative status. Moreover, its level remains stable in the actively cycling cells, implying that cancer cells engage in trogocytosis with NLCs between successive cell divisions. Analysis of the LNs from CLL patients reveals, for the first time, the presence of FOLR2$^+$ NLCs, whose frequency correlates with increased proliferation of cancer cells, and allowed detection of FOLR2$^+$ CLL cells, providing evidence of trogocytosis between NLCs and CLL cells in vivo. Finally, it proposes FOLR2 as a novel marker of M2-like NLCs *in vitro* and discovers a presence of heterogenous subpopulations of NLCs in the CLL lymph nodes, with varying expression of CD163 and FOLR2. These results shed light on the underappreciated role of trogocytosis in the increasing adaptability of malignant cells in the tumor microenvironment (TME) context and stress the importance of NLCs in the pathophysiology of CLL.

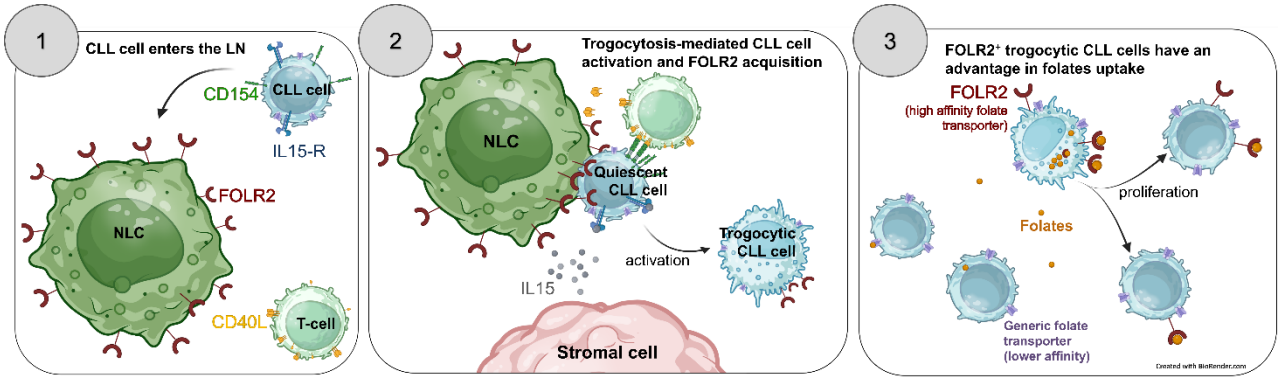

Schematic representation of trogocytosis-mediated acquisition of NLC-derived FOLR2 by CLL cells as a novel mechanism of cancer cell's interaction with TME and adaptation to the adverse conditions. 1) CLL cells enter the lymph node (LN) and engage in contact with FOLR2$^+$ NLCs. 2) Presence of T cells presenting CD40L and stromal cells producing IL-15 promotes the activation and trogocytosis-mediated acquisition of FOLR2 by CLL cells. FOLR2+ trogocytic CLL cells show increased acquisition of folates and are more likely to proliferate, as compared with the remaining population of cancer cells.

INTRODUCTION

Chronic lymphocytic leukemia (CLL) is the most common B cell malignancy of western countries, characterized by the clonal accumulation of dysfunctional, CD5$^+$ mature-like B cells in peripheral blood (PB) and lymphoid organs such as the bone marrow (BM) or lymph nodes (LNs)[1]. While in the periphery, CLL cells become quiescent, and in order to proliferate they migrate to lymphoid organs, especially LNs. LNs facilitate CLL cells interactions with their specific microenvironment[1]and represent the main site of

cancer cells proliferation[2]. Beside allowing their proliferation, the CLL microenvironment is also critical for cancer cell survival and chemoresistance[3–7] via a complex dialogue with T cells, endothelial cells, mesenchymal stromal cells and nurse-like cells (NLCs)[1,8]. NLCs were first observed in the long-term *in vitro* cultures of PBMC from CLL patients, and described as a monocyte-derived population of large and adherent cells interacting closely with CLL cells [9,10]. Further, NLCs were characterized as $CD68^+$ CLL-specific tumor-associated macrophages (TAMs), displaying M2-like phenotype with high expression of CD14, CD163, CD209[10–13] and low expression of M1-like markers such as CD64 and CD86[13]. NLCs participate in all the major steps of CLL survival and adaptation, and they are one of the main sources of CXCL12 (SDF-1) and CXCL13, chemokines that attract cancer cells to the lymphoid organs[1,8]. Soluble factors like CXCL12, BAFF, APRIL [1,8] and BDNF[14] expressed by NLCs support survival of CLL cells upon their tissue entrance. Moreover, vimentin and calreticulin presented by NLCs, serve as antigens recognized by CLL cells B cell receptors (BCRs), inducing their activation, and in turn survival and potentially, their proliferation[8,15]. Furthermore, NLCs participate in establishing and maintaining an immunosuppressive tumor microenvironment (TME) by inducing Treg expansion[16]. Increased numbers of NLCs in the LNs and their infiltration into proliferation centers are correlated with more aggressive disease[5] and shorter overall survival[5,17]. Moreover, NLCs protect CLL cells from therapeutic attacks. They are implicated in decreasing the proapoptotic effect of Ibrutinib[18], and render CLL cells less sensitive to Venetoclax, by release of BAFF[19] and WNT5[20], and to Fluradabine, by CXCL12 expression[21].

While the secretome of NLCs is widely recognized as playing an important role in the protective effect of NLCs towards CLL cells[6,8], there is growing evidence stressing the importance of intercellular interactions between NLCs and CLL cells in this aspect. Direct contact between NLCs and CLL cells mediated through CD31/plexin B on NLCs and CD38 on CLL cells is implicated in proliferation of $CD38^+/CD100^+$ malignant clones[22]. Moreover, our group showed that trogocytic interaction, partially mediated through CD2/CD58 (LFA-3) is essential in promoting cancer cell survival *in vitro*[23]. Trogocytosis is a peculiar mechanism of intercellular contact in which one cell interacts with and "gnaws" another, leading to the rapid acquisition of cellular content, including integral plasma membrane fragments[24]. This process is predominantly unidirectional, enabling the recipient cells to acquire new functionalities, among other things. Trogocytosis is an evolutionary-conserved process, implicated in both physiology and pathology [24–26]. However, its role in cancer, including CLL, especially in the context of malignant cell interactions with TME remains poorly understood[27].

In recent years, folate receptor β (FRβ/FOLR2) emerged as a specific marker of TAMs [28–30]. FOLR2 belongs to the family of the folate receptors, along with FOLR1, FOLR3, and FOLR4. Both FOLR2 and FOLR1 show high affinity for folates, but while FOLR1 is present on cells of epithelial lineage, FOLR2 expression is restricted to myeloid cells, particularly the M2-like immunosuppressive subpopulation of macrophages[31]. FOLR2 is mostly found in TAMs and some tissue-resident macrophages and is only present in low levels of a non-functional form on circulating monocytes, while being absent in M1-like macrophages. FOLRs along with two other receptors (RFC and PCFT) are the main receptors responsible for uptake of folates (vit. B9)[32]. FOLRs allow the cell an efficient uptake of folates, thanks to their very high affinity and quick internalization/recycling period[32]. Folates, including synthetic folic acid and its reduced physiological form 5-methyltetrahydrofolate, are essential co-factors for one-carbon metabolism, necessary for nucleic acid synthesis, amino acid homeostasis, epigenetic modifications and redox defense[33].

Our preliminary results on characterization of the NLC phenotype revealed a high expression of FOLR2 by these cells. The aim of this study was to evaluate the link between FOLR2 expression and the protective effect of NLCs on CLL cells, and deciphering a potential involvement of FOLR2 in the interaction between NLCs and CLL cells. We showed for the first time that NLCs express high levels of FOLR2, which serves as a distinctive marker of the protective phenotype of these cells. Furthermore, FOLR2 expression on NLCs correlates with the survival of cancer cells *in vitro*. Moreover, we demonstrated that CLL cells engage in trogocytic interactions with NLCs, leading to acquisition of functional FOLR2. As a result,

trogocytic FOLR2$^+$ CLL cells show increased capacity for folate uptake, and are found enriched in the fraction of activated and proliferating cells *in vitro*. Finally, we discovered a FOLR2$^+$ subpopulation of NLCs and the presence of trogocytic FOLR2$^+$ cancer B cells in the lymph nodes of CLL patients, confirming the relevance of this mechanism *in vivo.* These results stress the importance of trogocytosis in the NLC-CLL interactions, while FOLR2 acquisition by CLL cells represents a novel mechanism of NLC-mediated support of malignant B cells.

MATERIALS AND METHODS

Patient samples

Sample Collection and Informed Consent

Peripheral blood samples from CLL Patients were obtained from the Hematology Department with informed consent and referenced in the INSERM cell bank. According to French law, the INSERM cell bank has been registered with the Ministry of Higher Education and Research (DC-2013-1903) after being approved by an ethics committee (Comité de Protection des Personnes Sud-Ouest et Outremer II). Clinical and Biological annotations of the samples have been reported to the Comité National Informatique et Liberté.

Sample processing

Blood samples were collected from previously untreated patients (if not stated otherwise). PBMC from CLL patient's blood were isolated by density-gradient centrifugation on Ficoll-PaqueTM PLUS (GE Healthcare, Sweden). A fraction of the cells was used freshly for autologous CLL culture, CLL cells isolation or flow cytometry analysis. Remaining cells were frozen in Cryostor CM10 (STEMCELL Technologies, France) and stored in -80°C (short term) or liquid nitrogen (long term) until further use.

Cell isolation

CLL cells were isolated from fresh or frozen PBMC, using a EasySep™ Human B Cell Enrichment Kit II Without CD43 Depletion negative selection kit (STEMcell, France), according to manufacturer's protocol. Purity and viability of the cells after isolation were measured by flow cytometry following staining with CD5/CD19 antibodies and Annexin-V/7-AAD respectively. For each experiment, both values exceeded 95% (data not shown).

Healthy donor monocytes – following a buffy coat processing (EFS - Établissement français du sang, France), PBMC were subjected to CD14 MicroBeads positive selection kit with use of MS/LS columns (Miltenyi Biotec, France), according to the manufacturer's protocol. Eluted cells were stained with anti-CD14 mAb and analyzed by flow cytometry confirming >95% purity of the cells (data not shown). Isolated monocytes were used freshly for generation of monocyte-derived macrophages (MDM) or healthy donor NLCs (HD-NLCs).

Cell cultures

In vitro cultures were conducted using complete medium, composed of RPMI 1640 with GlutaMAX (Gibco, France), supplemented with 10% fetal bovine serum (FBS, Life Technologies, France) and 100 µg/ml of penicillin/streptomycin (Sigma-Aldrich, France). For experiments with varying concentration of folic acid (FA), media were prepared on the basis of RPMI 1640 without folic acid (Gibco, France) and 100 µg/ml of penicillin/streptomycin. For FA^{high} condition,

the media was supplemented with FA up to standard concentration of 2.27µM. Subsequently, both FA^{high} and FA^{low} media were supplemented with 10% FBS. For $FA^{negative}$ condition, 10% of dialyzed FBS (Sigma, Germany) was used instead. Cells were plated in tissue culture-treated plates (Corning, USA) at varying volumes: 4 mL per well for 6-well plates, 1.5 mL per well for 12-well plates, and 500 µl per well for 48-well plates. All cultures were maintained at 37°C in a humidified atmosphere with 5% CO2.

Freshly isolated CLL PBMCs were plated at a concentration of 10×10^6 cells/mL and maintained for up to 15 days. For analysis of CLL cells, the cells were collected by thorough pipetting, to collect both floating and loosely adherent cancer cells. For NLCs analysis, the remaining adherent cells were washed twice with phosphate-buffered saline (PBS) and treated with Accutase. After a 30-minute incubation at 37°C on an orbital shaker in the cell culture incubator, the cells were mixed with FBS and detached using a 16 cm cell scraper (Sarstedt, USA). Both floating and adherent fractions of the cells were combined for the NLCs analysis.

Monocyte-derived macrophage generation. Isolated CD14+ cells were plated at 0.5×106c/mL in the complete culture medium with 25 ng/mL of CSF1 or 50 ng/mL of GM-CSF to obtain M2- or M1-MDMs respectively. CSF-1 and GM-CSF were added again on day 3. On day 6, half of the culture medium was replaced with a fresh one, containing IL-4 and IL-13 to the final concentration of 25 ng/mL for M2 polarization and IFNγ at 100U, and 10ng/mL of LPS the day after for M1 polarization. Cells were polarized for 48h.

Healthy-donor NLC (HD-NLC) co-culture system
Experiments were performed using 48-well plates, using 500uL as a final volume of the culture.
Basic protocol:
CD14+ healthy donor monocytes at 0.5×10^6 c/mL were mixed with naïve purified CLL cells at 10x106c/mL in 500 µL of complete medium. After 10 days of co-culture, cells were activated with either a CpG + IL-2 cocktail or a CD40L + IL-15 cocktail for 72h and CLL cells were analyzed by flow cytometry.
Optimized Protocol:
First, MDMs were generated by culturing CD14+ cells at 1×10^6 cells/mL in 250uL of complete medium with 20ng/mL of CSF-1. After 6 days, the medium was replaced, and purified naïve CLL cells were added at a density of 6×10^6 c/mL in 250 µL of complete medium. 3 days later, 250ul of fresh medium with CD40L to a final concentration of 25ng/mL was added to the co-cultures. 2 days after the first activation, 300 µL of the medium was replaced, and cells were further activated with CD40L and IL-15 to final concentrations of 50 ng/mL and 25 ng/mL, respectively. 6 days post-second activation, cells were analyzed by flow cytometry.

FOLR2 gene KO in hNLCs with RNP Crispr-Cas9

Gene KO in HD-NLCs cultures were achieved using ribonucleoprotein (RNP)-mediated CRISPR-Cas9 gRNA method, using predesigned crRNA sequences (https://eu.idtdna.com/site/order/designtool/index/CRISPR_PREDESIGN), provided by Integrated DNA Technologies (IDT). For the target gene, three different crRNA targeting both alleles of the coding regions gene were used. Before each experiment, freshly isolated or frozen human monocytes were activated with 25 ng/mL of CSF-1 and cultured in the complete medium without antibiotics. $CD14^+$ monocytes were used 16h after isolation. At the day of electroporation, RNP complexes were prepared, according to protocol provided by IDT and Thermo Fisher. Briefly, crRNA and tracrRNA were reconstituted in IDTE buffer (IDT, USA). Then crRNA:tracrRNA duplexes were mixed in equimolar concentrations, followed by heating at 95°C for 5 min. Generated duplexes (gRNA) were used freshly, or were stored at -20°C for up to 6 months. Then each gRNA was mixed with Cas9 protein at a 1:1.2 molar ratio, incubated at 37°C for 20 min and equilibrated to RT. Pre-activated monocytes were detached, resuspended in buffer T and mixed with RNP complexes. Up to 5×10^6 cells were used per electroporation at 100µl, using Neon Transfection System, with a single pulse at 1900V and 20ms. Following electroporation, cells were plated in the complete medium. 90 min later, the cell culture media was replaced with a fresh one containing 20 ng/mL of CSF-1 to remove the traces of electroporation buffer. Afterward, cells were cultured for 5 days, before starting the co-culture with CLL cells or evaluating effectiveness of gene KO by qPCR or flow cytometry.

Flow cytometry

Extracellular staining:

All tested samples were resus, pended in the staining buffer (5% FBS, 0,5% of BSA, 2mM EDTA, 0.1% of sodium azide in PBS), supplemented with 2.5 µg/mL of Human BD Fc Block™ (BD Pharmingen, France) and 1% of human serum to prevent the non-specific antibody binding, and incubated for 15 min at 4°C. Subsequently, cells were stained with antibodies at saturating concentrations, for 20 min at 4°C. After washing, cells were re-suspended in PBS, containing 0.8 µg/mL 7-AAD (Sony, USA).

Intracellular staining:
Cells were stained with FVS620 viability dye (BD) according to manufacturer's protocol. Following the extracellular staining, cells were fixed and permeabilized with True-Nuclear™ Transcription Factor Buffer Set (Biolegened). Next, cells were stained with anti-Ki67 mAb (Invitrogen).

AnnexinV/7-AAD staining of CLL cells:
Cells were washed and resuspended in Annexin-V buffer and stained with Annexin-V-FITC (Miltenyi, Germany) according to manufacturer protocol. 5 minutes before the analysis, cells were re-suspended in Annexin-V buffer containing 0.8 µg/mL 7-AAD.

Following each staining, cells were immediately analyzed by flow cytometry (LSRII or FortessaX20, BD Pharmingen, France).

Results analysis:
All flow cytometry results were analyzed using FlowLogic 7.00.2 software (Inivai Technologies). Gating strategies for the analysis of CLL cell activation and proliferation can be found in the supplement section (Fig. S4D and S5A, respectively). Setting-up of the gates for the FOLR2$^+$ cells were set either based on isotype controls (Fig.2) or FMO controls (Fig. 4 and 5).
The analysis of the enrichment of FOLR2$^+$ trogocytic cells in the population of activated CLL cells, was made by introducing a FOLR2 enrichment score (ES_{FOLR2}), further correlated with the total percentage of CLL cells positive for a specific activation marker (Fig. S4E; A). Ki67 enrichment score was calculated analogously, to represent enrichment of Ki67$^+$ CLL cells in the population of FOLR2$^+$ trogocytic CLL cells.

Fluorescence microscopy imaging

Following the long-term culture (12-14 days), CLL PBMC were harvested and re-suspended in the staining buffer (5% FBS + 0.5% of BSA + 1mM EDTA in PBS) containing 1% of human serum and 2.5 µg/mL of Human BD Fc Block™ (BD Biosciences, France) and incubated for 15 min at 4°C. For detection of extracellular antigens, cells were directly stained with fluorochrome-conjugated antibodies anti-CD19 (Sony) and rabbit anti-FOLR2 mAbs (Abcam) for 20 min at 4°C. Subsequently, cells were washed x4 with PBS and fixed with 4% PFA in PBS for 20 min at RT. Following washing, cells were counterstained with DAPI (1µg/mL) for 5 min, washed with PBS and left on the cover glass O/N at 4°C to facilitate attachment of the cells. The next day, slides were mounted using Fluoromount media (ThermoFisher), and imaged using confocal microscope LSM 780 or 880 (Zeiss).

Trogocytosis assay

Autologous or heterologous NLCs were detached using Accutase and stained with PKH67 according to the manufacturer's protocol. Next, stained NLCs were mixed with naïve CLL cells after negative selection (ratio 1:3), transferred to 96-well Ultra-low attachment (ULA) plate and placed in the cell culture incubator at 37°C for 3 hours. Afterward, cells were stained with appropriate antibodies and analyzed by flow cytometry. We used purified naïve CLL cells, as the negative control of trogocytosis.

Immunohistochemistry

FOLR2 Immunohistochemistry

Automated classical immunohistochemical (IHC) stain was performed using the BOND RX automated slide stainer (Leica Biosystems, France). Slides (4µm) were deparaffinized and heat-pretreated using the ER2 solution (pH8) during 20 min. After peroxidase blocking, slides were incubated with the rabbit primary anti-FOLR2 antibody, clone EPR25731-70 (ABCAM Netherlands, at final dilution of 1/200, Envision Flex antibody diluent, Agilent Technologies) for 15 minutes. The target is visualized using the BOND Refine DAB detection kit (DS9800, Leica Biosystems, France). Slides were counterstained using Hematoxylin (Leica Biosystems, France), dehydrated and mounted using a xylene-based mounting medium (Sakura TissueTekÒ, Sakura FineTec France).

Multiplex Immunofluorescence (mIF)

The BOND RX staining platform (LEICA Biosystems, Germany) was used to automate the mIF staining procedure on 4 µm FFPE tissue sections. After baking and dewaxing, tissue slides were heat-pretreated for 20 min at 100°C using ER2 pretreatment solution (pH9, LEICA Biosystems, Germany). The slides were blocked for endogenous peroxidase activity using the Discovery inhibitor (15 minutes at room temperature) (07017944001, Roche Diagnostics, Switzerland). The slides were then stained for 5-plex immunofluorescence using the OPAL™ Technology (AKOYA Biosciences, USA) with sequential denaturation using ER1 pretreatment buffer (pH6, LEICA Biosystems, Germany), for 20 min at 97°C between each antibody-staining cycle. Primary antibodies were applied and incubated during 30 min at room temperature programmed in the aforementioned staining cycles in the following order: FOLR2 (clone EPR25731-70 (ABCAM Netherlands), at final dilution of 1/200, Envision Flex antibody diluent, Agilent Technologies), Ki67 (clone SP6, Ready to use, Zytomed, by Diagomics, France), CD163 (clone MRQ-26, Ready to use, Roche Diagnostics), CD68 (clone PGM-1, at dilution of 1/100, in Envision Flex antibody diluent) and CD20 (clone L26, Ready to use antibody diluted at ¼ in Ventana Antibody diluent, Roche Diagnostics). Subsequently, slides were incubated using the Opal polymer HRP detection system, allowing for OPAL™ dye precipitation. Five OPAL™ dyes with excitation and emission wavelengths compatible with our whole slide imaging system were used: OPAL™ Polaris 480, OPAL™ 520, OPAL™ 570, OPAL™ 620 (1/300 in 1x Plus Automation Amplification Diluent, AKOYA Biosciences, USA) and OPAL™ 690 (1/150 in 1x Plus Automation Amplification Diluent). The tissue slides were counterstained using Spectral DAPI (AKOYA Biosciences, USA) and mounted with Invitrogen™ ProLong™ Gold Antifade Mounting medium (Life Technologies, USA).

Image analysis

The mIF images were analyzed by HALO software (version 3.6, Indica Labs, USA). Briefly, each section was manually annotated, to take into consideration the maximal area of the tissue, with removing the artifacts generated during the sample preparation. Subsequently, we optimized the segmentation parameters, allowing for the most consistent cell separation, adjusting each marker to minimize the false positive events. Afterward, the annotated regions were segmented and analyzed, and obtained image data was exported as FCS file, for subsequent analysis by FlowLogic software. Each cell was classified based on the combination or the specific dye intensity and the completeness of their nuclei or cytoplasmic region.

Statistical analysis

All statistical analyses were performed using Graph Pad Prism 10.1.2. Mann-Whitney U test was used for comparison of MFI of surface markers on NLCs and other macrophages. Paired t-test or Wilcoxon test was used to determine the differences in viability of CLL cells or MFI. One-way ANOVA with Geisser-Greenhouse correction was used to compare the results of analyzes on CLL cell viability, activation, and proliferation. Results in the bar plots are presented as mean ± SD. The lines in the middle of the boxes in the box-and-whisker plots represent median values. The p-values below 0.05 were considered statistically significant.

RESULTS

FOLR2 expression by NLCs is correlated with the *in vitro* survival of CLL cells

The polarization state of TAMs is determining for their role in the TME[34]. We have previously demonstrated that M2-like NLCs (CD163^{high}, CD14^{high}, CD209^{pos}, CD64^{low}, CD86^{low}) are able to interact with CLL cells and to support them, contrary to M1-like NLCs (CD163^{low}, CD14^{low}, CD209^{low}, CD64^{high}, CD86^{high})[13]. To further define protective NLCs, we tested their expression of some recent surface markers associated with M2-like TAMs, including: MerTK, MARCO, B7-H4, VSIG4, CD36, VISTA, CD369, GPNMB and FOLR2. The screening of these molecules revealed that only FOLR2 was highly expressed by NLCs (Fig. S1A and 1A). Additionally, we observed that FOLR2 was co-expressed along CD163, a standard marker of NLCs[5] [Fig. S1B]. Expression of FOLR2 is limited to a narrow subpopulation of myeloid cells, mostly CSF-1 activated M2-like macrophages and TAMs[35]. In this regard, NLCs showed a significantly higher expression of FOLR2 as compared with M2-like and M1-like monocyte-derived macrophages (M2-like and M1-like MDMs; Fig. 1A).

Having realized the potential importance of this marker, we characterized the kinetic of FOLR2 expression in monocyte differentiation into NLCs during 14 days of PBMC *in vitro* culture. The FOLR2 signal was detectable on CD14^{+} cells from day 3, and for patients P1-3 reached maximum level between days 9-10, corresponding to the appearance of mature NLCs, while for patients P4-6 it diminished completely towards the end of the culture (Fig. 1C). Interestingly, for P1-3 (FOLR2^{high}) CLL cells survival on day 14 exceeded 90%, whereas for P4-6 (FOLR2^{neg}) it was below 65% (Fig. 1D). Next, we further investigated the relationship between FOLR2 expression on NLCs and CLL cell survival *in vitro,* in 62 patient samples. Based on FOLR2 expression on NLCs, we categorized PBMC cultures into three groups: FOLR2^{high}, FOLR2^{low} and FOLR2^{neg} (Fig. S1C). The CLL cell survival among these three groups showed a significant difference, being highest in the FOLR2^{high} group and the lowest in the FOLR2^{neg} group (Fig. 1E). To confirm that increased survival of CLL cells from the FOLR2^{high} group is dependent on NLCs, we compared the viability of CLL cells cultured alone (CLL cells after negative selection) or with other PBMCs (containing NLCs). As a result, we observed a significantly increased survival of cancer cells only with NLCs from the FOLR2^{high} group, but not for the FOLR2^{neg} group (Fig. S1D). These results demonstrate that NLCs expressing FOLR2 can protect CLL cells from spontaneous apoptosis *in vitro*.

Next, we compared the correlation between survival of cancer cells in the PBMC culture with expression of FOLR2 and other myeloid markers by NLCs (Fig. 1F). Based on the results from 40 patient samples, we observed the highest correlation with cancer cell survival for FOLR2 (detailed results on Fig. S1E), followed by M2-like markers CD163 and CD14. The CD206 expression on NLCs was not significantly correlated with survival of the CLL cells, while CD64 and CD86, M1-like markers of macrophage polarization, showed a negative association with cancer cell survival. These results indicate that FOLR2 is a very specific and consistent marker of protective M2-like NLCs *in vitro*.

Finally, we evaluated the FOLR2 expression by NLCs in the lymph nodes (LNs) of CLL patients. First, we compared the presence of FOLR2$^+$ macrophages in the non-malignant, reactive LNs with LNs from CLL patients. Multiplex Immunofluorescence (mIF) staining revealed a markedly higher expression of FOLR2 by CD163$^+$ macrophages in the CLL LNs, compared with the non-malignant ones (Fig. 1G; Fig. S1F for the quantification). Furthermore, following analysis of 25 CLL patient samples (Table 1), we observed a high prevalence (>60%) of FOLR2$^+$ cells among population of NLCs in most of the cases (22/25), including the patients with Richter's transformation (3/3), accelerated disease (13/14), and after previous treatment (7/7). Detection of FOLR2$^+$ NLCs in the LNs from patients with various stages of CLL suggests that these cells might play an important role during all stages of the disease.

FOLR2 is detected on CLL cells co-cultured with NLCs

Considering that CLL cells drive maturation of NLCs, and that NLCs express a high level of FOLR2, which correlates with survival of cancer cells *in vitro*, we wondered if FOLR2 could play a role in the interaction between these two cell types. The first clue of the potential involvement of FOLR2 in the interaction between NLCs and CLL cells came from routine phenotyping of NLCs in PBMC cultures by flow cytometry. As expected, we observed a high expression of myeloid markers: FOLR2, CD163, CD206 and CD14, on the big granular cells corresponding to NLCs (Fig. 2A, Fig. S2A for the full gating strategy). Surprisingly though, when gating on the small events corresponding to lymphoid cells (composed mainly of CLL cells), we detected a fraction of lymphoid cells positive for FOLR2 and, to a lesser extent, CD14 (Fig. 2A). The analysis of samples from 19 patients confirmed that only FOLR2, among the tested myeloid markers, was significantly detectable on the lymphoid cells (Fig. 2B). Subsequently, we conducted a similar analysis, focusing directly on the population of CD5$^+$/CD19$^+$ cancer cells. We confirmed that FOLR2 is absent on naïve CLL cells, immediately after isolation from blood, and appears only after long-term PBMC culture (Fig. 2C). Interestingly, qPCR analysis of RNA isolated from purified cancer cells from these two types of cultures did not detect any *FOLR2* gene expression (Fig. S2B).

Taken together, these observations suggested that CLL cells acquired FOLR2 during PBMC cultures, with NLCs being the most plausible source. To confirm whether CLL cells could acquire FOLR2 from NLCs, we performed *FOLR2* gene KO in NLCs. To generate sufficient NLC cells to test this hypothesis, we used a healthy donor NLCs system (HD-NLCs), where CD14$^+$ monocytes from healthy donors (HD) are co-cultured with purified, naïve CLL cells. These HD-NLCs correspond to NLCs in terms of functionality[10] and FOLR2 expression (Fig. S2C). The efficacy of *FOLR2* KO in HD-NLCs is shown in Fig. S2D. Flow cytometry analysis of CLL cells cultured with *FOLR2* KO HD-NLCs showed a substantially reduced level of FOLR2 signal on cancer cells as compared with the control condition (Fig. 2D, left panel), which was further confirmed with 11 biological replicates (Fig. 2D, right panel). These results demonstrate that NLCs are the source of the FOLR2 detected on CLL cells in the *in vitro* PBMC cultures.

CLL cells acquire functional FOLR2 from NLCs through trogocytosis

Having identified NLCs as the most likely sources of FOLR2 on CLL cells, we aimed to identify the mechanism responsible for the FOLR2 transfer from NLCs to CLL cells. We can distinguish several ways in which intercellular protein exchange can take place, including exosomes, nanotubes and trogocytosis[36]. Out of the three, the last one seemed the most plausible, as we have shown previously that CLL cells can acquire plasma membrane fragments from NLCs by trogocytosis[23]. To demonstrate the direct cell interaction between NLCs and CLL cells, we stained NLCs with PKH67, a stable membrane dye, and co-incubated them with purified naïve CLL cells for 4h at 37°C. Analysis of CLL cells by flow cytometry revealed a population of PKH67$^+$ cells that were partially positive for FOLR2, but not for CD14 and CD16 (Fig. 3A). Across 15 samples, a mean of 20% and 2% of CLL cells were positive for PKH67 and FOLR2 respectively, while the signal from CD14 and CD16 was absent (Fig. 3B). These results further demonstrate that CLL cells obtain FOLR2 directly from NLCs and that the transfer is partially selective.

To further characterize the CLL-NLC interaction, we visualized the long-term PBMC cultures by confocal microscopy. Figure 3C shows a 3D-projection of NLCs stained extra- and intracellularly with anti-FOLR2 mAb (red), in tight contact with CLL cells stained with anti-CD19 mAb (cyan). While focusing on the planes with cancer cells alone, we observed some CLL cells with FOLR2 staining in the form of singular patches co-localized with CD19 on the plasma membrane (Fig. 3D and S3A), which is one of the hallmarks of trogocytosis. To further test the transfer of FOLR2 from NLCs to CLL cells, we performed co-cultures of purified naïve CLL cells with *FOLR2* KO HD-NLCs. We observed no signal of FOLR2 on CLL cells co-cultured with *FOLR2* KO HD-NLCs as compared with the control conditions (Fig. 3E), further confirming that NLCs are the source of the FOLR2 detected on cancer cells.

Having established the transfer of FOLR2 protein from NLCs to CLL cells, we tested whether the FOLR2 acquired by CLL cells was functional and could transport folates. To study the folate uptake, we incubated the HD-NLCs-CLL cell co-cultures for 80 min with EC17, a folic acid-FITC imaging agent[37], and then analyzed the cells with confocal microscopy. As expected, NLCs showed high surface FOLR2 (red) and intracellular EC17 (green) signals. As for CD19$^+$ CLL cells, we observed some with FOLR2 positive membrane patches and intracellular EC17 signal (Fig. 3F, top). On the other hand, CLL cells co-cultured with *FOLR2* KO NLCs lacked the FOLR2 signal and showed greatly reduced EC17 signal (Fig. 3F, bottom panel). To rule out the effect of direct transfer of EC17 from NLCs to CLL cells, which we observed previously upon live-imaging experiments (Fig. S3B), we performed the analogous co-culture as in fig. 3F, but before EC17 incubation, we purified the CLL cells by negative selection. In this case, we observed EC17$^+$ CLL cells following the co-culture with control NLCs, but not with *FOLR2* KO NLCs (Fig. 3G). Finally, with flow cytometry analysis, we observed an elevated acquisition of the folic acid probe by the FOLR2$^+$ population of CLL cells (Fig. S3C).

To summarize, the presented results confirmed that CLL cells obtain FOLR2 from NLCs via trogocytosis. Furthermore, acquired FOLR2 is functional and facilitates the uptake of folic acid by cancer cells.

FOLR2 acquired by CLL cells from NLCs correlates with their activation status

After confirming that CLL cells acquire functional FOLR2 from NLCs through trogocytosis, we sought to investigate the potential benefits of this process for cancer cells, as well as to identify the optimal conditions to maximize it. First, we evaluated the effect of *FOLR2* KO in NLCs, on the CLL cell survival and activation, using the HD-NLCs co-culture system. Surprisingly, we observed no changes in either viability or expression of positive (CD23) and negative (CD184) activation markers by cancer cells, regardless of the presence of folic acid in the medium (S4A). Considering that *in vivo* CLL cells could engage in trogocytosis with NLCs in lymphoid organs, where they interact with other elements of the TME leading to their activation and proliferation, we attempted to mimic these conditions using soluble factors. We chose two priming protocols (Fig. S4B) to reproduce lymph-node conditions *in vitro*: first, we used CpG+IL-2[38], for TLR-centric activation, where CpG substitutes the danger signal, and IL-2 mimics the presence of T cells; second, with CD40L[1]+IL-15[38,39] for a more BCR-centric activation of CLL cells, where CD40L mimics T helper cells and IL-15 accounts for stromal[40] and dendritic cells[41]. Analysis of CLL cell cultures treated with soluble factors demonstrated that CpG+IL-2 activation leads to a significant increase of CD23 levels in both monocultures and co-cultures with HD-NLCs (Fig. 4A). In contrast, CD40L+IL-15 treatment induced a strong upregulation of CD23 and downregulation of CD184, but only in the presence of HD-NLCs. Moreover, CD40L+IL-15 priming led to significant increase of FOLR2 acquisition by CLL cells as compared with untreated and CpG+IL-2 conditions (Fig. 4B). Next, we tested the effect of increasing the number of HD-NLCs in the culture on FOLR2 acquisition by CLL cells. We observed a significant increase of FOLR2 uptake by CLL cells upon raising the percentage of HD-NLCs in the co-cultures from 5 to 10%, while 20% did not yield further changes (Fig 4C).

Since CD40L+IL-15 treatment led to NLC-dependent activation and increased FOLR2 acquisition by CLL cells, we used it for subsequent investigation of the trogocytosis process in cancer cells. To further maximize the FOLR2 trogocytosis by cancer cells, we increased the number of HD-NLCs in the co-cultures to 10% and incorporated additional cytokine priming and medium exchange to minimize the effects of nutrient depletion (Fig. S4C). We used these optimized culture conditions, with CD40L+IL-15 stimulation for all the subsequent experiments. Besides CD23 and CD184, we analyzed additional markers of CLL activation: CD49d, associated with CLL aggressiveness[42] and resistance to treatment[21]; CD58, a molecular partner in CLL-NLC cell-cell contact[23]; and CD71, a general marker of cell activation and proliferation[43]. With the optimized protocol, we confirmed increased expression of activation markers: CD23, CD49d, CD58, CD71, and a decreased expression of CD184 by CLL cells co-cultured with HD-NLCs, as compared with CLL cells cultured alone (Fig. 4D). Furthermore, we observed a significantly increased frequency of $FOLR2^+$ trogocytic CLL cells, reaching 70%, with a median level of ~40% (Fig. 4E), representing roughly 10-fold increase as compared with our previous experiments using a basic activation protocol (Fig. S4B). Aside from intensification of the FOLR2 trogocytosis by CLL cells, the CD40L+IL-15 treatment led to the acquisition of other myeloid markers by cancer cells, CD11b and CD14 (Fig. S4F). Plotting FOLR2 signal against CLL activation markers demonstrated that the $FOLR2^+$ cell population is more likely found in the activated fraction of the cells, with high expression of CD23, CD71, CD49d, CD58 and low expression of CD184 (Fig. 4F). We further supported these findings, by confirming a strong correlation between FOLR2 enrichment score (ES_{FORL2}) and the total % of CLL cells positive for a specific activation marker (Fig. 4G).

Taken together, these results demonstrate that CD40L+IL-15 stimulation greatly promotes trogocytosis of FOLR2 by CLL cells, and that FOLR2$^+$ trogocytic cancer cells are enriched in the fraction of activated cells.

FOLR2 acquisition by CLL cells correlates with their proliferation

Following the discovery of a link between FOLR2 trogocytosis and the activation of CLL cells, we aimed to explore the connection between this phenomenon and CLL cell proliferation. To this end, we compared the expression of Ki67 in CLL cells cultured in the presence of CD40L + IL-15 alone or in the presence of HD-NLCs. Flow cytometry analysis demonstrated that CLL cells cultured alone lack FOLR2 and Ki67 signal, while in the presence of HD-NLCs there is an induction of Ki67 expression, which is predominantly present on the FOLR2$^+$, CD23$^+$ and CD184^{low} subpopulation of CLL cells (Fig. 5A). The significant increase of Ki67 level in the presence of HD-NLCs was confirmed for 17 biological replicates (samples from 12 patients; Fig. 5B, Fig. S5B). We then analyzed the expression of Ki67 in terms of enrichment in the population of FOLR2$^+$ CLL cells following co-culture with HD-NLCs. The systematic comparison of the percentage of Ki67$^+$FOLR2$^+$ double positive cells among the total fraction of Ki67$^+$ CLL cells showed a strong correlation between the two parameters (Fig. 5C). Since expression of Ki67 is only transient and mostly specific to actively cycling cells[44], we also tested cellular proliferation by the dye-dilution assay with use of CellTrace™ Violet (CTV) dye. By following the evolution of the CTV signal on cancer cells (Fig. 5D, left), we demonstrated that CLL cells are indeed cycling in our experimental set-up, and confirmed that the phenomenon is significantly increased in the presence of HD-NLCs (Fig. 5D).

All previous experiments were performed in complete culture media, containing excess of folic acid (FA). To evaluate the effect of FA availability on CLL proliferation in the presence of HD-NLCs, we tested three culture conditions with decreasing FA content, a complete medium (FA_{high}; FA>1000µg/L), RPMI without FA + 10% FBS (FA_{low}~1.22µg/L) and RPMI without FA + 10% dialyzed FBS ($FA_{negative}$~0µg/L). Systematic analysis of Ki67 expression and CTV dilution in CLL cells from six selected patients revealed that scarcity of FA leads to significant decrease of cancer cell proliferation (Fig. 5D). Surprisingly, in FA^{low}, after 6 days of activation we still observed around 30% of Ki67 positive CLL cells vs 40% in FA^{high}, while in FA^{negative} this value was below 1%, signifying lack of actively proliferating cells (Fig. 5E, left). As for the CTV dilution assay, we confirmed that deprivation of FA causes significant decrease in CLL cell proliferation (Fig. 5E, right). Nevertheless, even in FA^{negative} conditions we still observed that around 20% of cancer cells had undergone cell division.

FOLR2+ trogocytic CLL cells are the predominant population of proliferating cancer cells under folic acid deprivation

To evaluate if trogocytic FOLR2$^+$ CLL cells have an advantage in proliferation during scarcity of FA, we combined the results of Ki67 and CTV staining and studied the distribution of FOLR2$^+$ cells in the subpopulation of actively cycling CLL cells. As an example, we chose a specific patient with highly proliferative cells, capable of multiple cell division over the course of the experiment (Fig. 5F). Based on CTV staining alone, we observed a diminishing number of CTV peaks following a decrease in FA content in the media, with 5 peaks in FA_{high}, 4 peaks in FA_{low} and only 2 peaks in $FA_{negative}$ conditions. When looking at

CTV and Ki67 signals combined, we could differentiate the four cell populations, corresponding to: P1. $CTV^{high}Ki67^{-}$: quiescent cells that did not divide; P2. $CTV^{high}Ki67^{+}$, cells right before the first division; P3. $CTV^{low}Ki67^{+}$: subsequent generations of actively cycling cells; P4. $CTV^{low}Ki67^{-}$: cells after cycling, quiescent again. Looking at FORL2 expression in these cells subsets, we observed the highest level in P2 with a slight decrease in P3, that is however consistently higher than that of P1 and P4. As for the CD23 marker, we observed low levels in P1 and P4, the highest level in P2, and a decrease in P3. The highest level of CD184 was observed for P1 and P4, followed by a gradual decrease in P2 and P3. These results suggest that $FOLR2^{+}$ CLL cells are the predominant population of actively cycling cells (P2, P3), which is especially pronounced in FA_{low} conditions. Finally, by analyzing the subsequent cell generations of actively cycling cells (P3) we observed a stable level of FOLR2 (Fig. 5G), indicating that these cells performed multiple rounds of trogocytosis, since FOLR2 levels drop proportionally after each cell division.

These experiments demonstrated that NLCs play a crucial role in IL-15/CD40L mediated CLL cell proliferation *in vitro*, and that $FOLR2^{+}$ trogocytic CLL cells are the predominant population of actively cycling CLL cells in HD-NLCs co-cultures. Furthermore, a stable level of FOLR2 in the actively dividing cell fraction indicated that CLL cells engage in trogocytosis after each cell cycle. Finally, cell cultures with decreasing concentration of FA confirmed that trogocytic $FOLR2^{+}$ CLL cells have a proliferative advantage under FA depletion compared to $FOLR2^{-}$ cancer cells.

Heterogeneity of NLCs and detection of trogocytic $FOLR2^{+}$ CLL cells in the lymph nodes of the patients

Previous *in vitro* experiments demonstrated that NLCs expressing FOLR2 are the main subpopulation of macrophages protecting CLL cells from spontaneous apoptosis, and that trogocytosis-mediated FOLR2 acquisition by cancer cells is associated with their activation and proliferation. In the next step, we aimed to investigate these phenomena in the LNs of CLL patients.

First, we took a closer look at the subpopulation of NLCs in the LNs of the patients. Based on FOLR2 and CD163 staining and the spatial distribution of NLCs, we detected 4 main subpopulations of these cells: P1 ($FOLR2^{+}/CD163^{+}$), P2 ($FOLR2^{+}/CD163^{-}$), P3 ($FOLR2^{-}/CD163^{+}$) found with varying frequency in sub-capsular areas and lymphatic sinuses, and P4 ($FOLR2^{+++}CD163^{++}$) located densely around the vascular structures (Fig. 6A). While the expression of both FOLR2 and CD163 by 4 subpopulations of NLCs varied significantly, the most pronounced difference was observed in case P4, for which FOLR2 MFI was consistently a few times higher as compared with remaining subtypes of NLCs (Fig.6A right).

Aside from $FOLR2^{+}$ NLCs, we also detected the presence of $CD20^{+}$ CLL cells with patches of FOLR2 signal in plasma membrane and cytoplasm of the cells (Fig. 6B), suggesting a presence of trogocytic cancer cells, previously observed *in vitro*. Some of these $FOLR2^{+}$ CLL cells were also $Ki67^{+}$. Nevertheless, the insufficient thickness of the slides did not allow for quantitative analysis of these cells in the tissue.

Since we could not confirm the enrichment of the trogocytic $FOLR2^{+}$ CLL cells in the fraction of proliferating cells, we investigated the potential relation between the frequency of $FOLR2^{+}$ NLCs (P1, P2 and P4) and the overall percentage of $Ki67^{+}$ CLL cells in the LNs. First, we noticed that the P1 and P2 subpopulations of NLCs are tightly intertwined with proliferating CLL cells (Fig. 6C). Then, we analyzed the LNs from 21 patients, and based on percentage of $Ki67^{+}$ cancer cells, we divided the samples into low and high proliferation groups with <10% $Ki67^{+}$ and >10% $Ki67^{+}$ CLL cells respectively (Fig. 6D). Comparison of the $FOLR2^{+}$ NLCs (P1, P2 and P4) percentage between these two groups revealed their significantly higher abundance in the samples with increased proliferation of CLL cells.

Observation of NLCs with heterogenous expression of FOLR2 and CD163 suggested a different specialization of these cells within the lymphoid tissue. Especially in case of FOLR2^{+++}CD163^{++} NLCs associated with vasculature. Moreover, observation of FOLR2^{+} CLL cells confirmed that trogocytosis with NLCs occurs *in vivo*. Finally, a positive association of the frequency of FOLR2^{+} NLCs with increased proliferation of CLL cells further enforced the importance of these cells in supporting cancer cell expansion.

DISCUSSION

Understanding the intricacy of intercellular communication between cancer cells and other players in the TME represents an essential challenge in further elucidating oncogenesis, therapy resistance, and ultimately developing more efficient therapeutic strategies for cancer control[45]. While the role of cytokines[46] and exosomes (EVs)[47] in cancer has been well established over the years, the direct cell interactions remain understudied. Although progress has been made in identifying several cell types involved in cell-cell communication and their underlying molecular mechanisms[48], tracking these events in tissues remains challenging, due to their elusive nature and technological limitations. In the current era of transcriptomic analyses, even at the spatial level, most of these events are irretrievably lost during the standard processing of the tissues or remain undetectable. This is especially true for mechanisms involving a direct exchange of the cellular content, whose detection often requires an a priori hypothesis, as they can otherwise be incorrectly dismissed as experimental artifacts. Therefore, further close characterization of the cells composing the TME as well as of their physical contacts with cancer cells, is needed to identify new direct cell-cell interactions with potentially important roles in cancer.

Direct contact with NLCs is a pivotal element in supporting CLL cells *in vitro*. In this context, trogocytosis was shown to be a critical factor in promoting cancer cell survival[23]. Here, using primary CLL samples, we demonstrate for the first time that malignant B cells acquire functional FOLR2, a myeloid-specific nutrient transporter, through trogocytosis-mediated interaction with FOLR2^{+} NLCs. As a result, FOLR2^{+} trogocytic CLL cells show increased capacity for folic acid uptake and are predominantly detected in the fraction of activated and proliferating cancer cells *in vitro*. Lu et al. demonstrated a similar phenomenon in the case of NK cells, that could acquire a tyrosine kinase receptor TYRO3 by trogocytosis, resulting in their increased activation and proliferation[49]. Furthermore, we detected FOLR2^{+} CLL cells in the LNs of CLL patients and confirmed a correlation between percentage of FOLR2^{+} NLCs and cancer cells proliferation. Both results support the relevance of trogocytosis-mediated acquisition of FOLR2 by CLL cells, and the importance of FOLR2 expressing NLCs *in vivo*.

From their discovery, NLCs were defined as CLL-specific TAMs with expression of CD14, CD68, CD86[10], and CD163[12]. Considering their heterogeneity *in vitro*, we previously established the protective phenotype of NLCs to be CD163^{high}, CD14^{high}, CD209^{high}, CD86^{low} and CD64^{low}[13]. Here we further defined the phenotype of NLCs, and present FOLR2 as the ultimate marker of NLCs, which alone allows to discriminate between protective and non-protective phenotypes. Moreover, we demonstrated that in the CLL LNs, FOLR2 is expressed by the majority of NLCs. With further analysis of CLL LNs, we revealed the presence of different subpopulation of NLCs varying in expression of CD163 and FOLR2, and observed that FOLR2 expressing subset of NLCs as highly intertwined with proliferating CLL cells. Moreover, we distinguished a population of NLCs highly associated with vasculature and characterized with especially high expression of FOLR2. We presume that this group of NLCs might be responsible for homing the CLL cells to the

lymphoid organs[1]. These results highlight previously unknown heterogeneity of NLCs, stressing the importance of further characterization of these peculiar cells.

While the FOLR2 expressing NLCs seem to be a crucial element of CLL TME, the exact role of FOLR2 in these cells as well as other TAMs remains speculative. According to the literature, expression of FOLR2 may lead to accumulation of folates in macrophages, supporting epigenetic changes that stabilize the immunosuppressive phenotype of these cells[32]. This stays in agreement with the results by Vaca et al., demonstrating that NLCs are highly immunosuppressive cells, promoting expansion of T helper cells, and further hindering immune responses against cancer cells[16]. Moreover, following the observation of folic acid transfer from NLCs to CLL cells, we speculate that FOLR2^{high} NLCs could act as a reservoir of folates for the cancer cells in the lymphoid organs. This could be especially relevant during the active phase of the disease, when the concentration of this vitamin might become a limiting factor for cell proliferation[32].

While *FOLR2* is exclusively expressed by a subpopulation of myeloid cells, here we demonstrated that it could be also actively acquired by cancer cells by trogocytosis. Thanks to its high affinity, and rapid turnover[31,35,50], FOLR2 gives the trogocytic cancer cells an edge over the rest of the cancer cells in the uptake of folates. Folates are essential fuel for one-carbon metabolism, impacting nucleic acid, lipids and amino acids synthesis, necessary for cell growth and proliferation[33]. This would be consistent with our observation that, aside from the direct increase in the folic acid uptake, FOLR2^{+} trogocytic CLL cells belong to the predominant population of activated and proliferating cancer cells *in vitro,* especially in conditions with decreased access to this vitamin. This suggests that trogocytosis-mediated interaction with NLCs, as well as the resulting FOLR2 acquisition by CLL cells, play an important role in the adaptation to decreased access to folates. Moreover, we demonstrated that the actively cycling population of CLL cells *in vitro* is characterized by a constant level of extracellular FOLR2, which drops as soon as they become quiescent again. This implies that CLL cells engage in trogocytosis with NLCs between each cell cycle and use FOLR2 to sustain their increased folate demands. These findings are supported by our observation that CLL cells remain in close contact with FOLR2^{+} NLCs in the CLL LNs, and that during CLL progression, NLCs show an increased infiltration into proliferation centers[5], hence being more accessible for the actively proliferating CLL cells.

Another interesting point to address is the observed selectivity of the protein transfer during the trogocytosis between NLC-CLL interaction. The observation that the protein transfer during NLC-CLL interaction is partially selective, and additionally depends on the cytokine treatment, could shed light on the potential extent of the trogocytic interaction. Out of the tested proteins, FOLR2 is the main NLC-derived protein detectable on CLL cells in the resting conditions. FOLR2 is a small, GPI-anchored protein located abundantly on the plasma membrane (PM) of NLCs. On the other hand, CD16, CD163 and CD206, which show negligible acquisition by CLL cells, are all integral transmembrane proteins, with stronger association to the PM. This suggests that, in resting conditions, trogocytosis encompasses only the outer layer of the NLC PM. On the other hand, CD14 is also a small GPI-anchored protein, predominantly co-expressed with FOLR2, yet showing much smaller transfer, and retention by CLL cells, which further indicates the selectivity and importance of FOLR2 transfer. We could speculate that CLL PM contains molecules that stabilize interaction with FOLR2, resulting in its higher acquisition and retention. Moreover, upon CD40L+IL-15 priming, we observed not only a 10-fold increase in the transfer of FOLR2 to cancer cells, but also a substantial acquisition of CD11b and CD14, suggesting that that this activation is intensifying interaction between CLL cells and NLCs, and thus the trogocytosis process itself. It has been shown previously that FOLR2 inhibits the CD11b/CD18-mediated adhesion of macrophages to collagen[51], and so it might be also implicated in regulating the interaction between NLCs and CLL cells.

Trogocytosis represents one of the most rapid and efficient mechanisms of intercellular transfer of various components, including proteins and lipids[24]. While our results clearly support a trogocytic

transfer of plasma membrane fragments from NLCs to CLL cells, we cannot completely rule out that another form of intercellular protein transfer like extracellular vesicles (EVs) or nanotubes could play a role in the pro-tumoral effect of the NLC-CLL cell interaction[52]. For instance, Ikhlef et al. demonstrated that NLC-derived exosomes have an anti-apoptotic effect on CLL cells, conferring them more resistant to Ibrutinib, and supporting their proliferation[53]. However, these findings contradict our previous observations, showing an abrogation of the protective effect of NLCs once separated from CLL cells by Transwells, that normally do not block EVs transfer[23]. As for nanotubes, it is a mechanism implicated more in transfer of cytoplasmic contents, rather than rapid acquisition of membrane fragments[54].

Nevertheless, the acquisition of FOLR2 by CLL cells cannot fully account for the beneficial effect of trogocytosis regarding cell activation and proliferation. Already, based on PKH67 staining we observed that FOLR2$^+$ CLL cells represent only a fraction of the total population of trogocytic cells, which acquire also other components of NLCs plasma membrane. Other researchers proposed that trogocytosis could help cells gain lipids necessary for cell proliferation[24], which is in line with our results. Especially regarding the observation that actively proliferating cells are engaging in trogocytosis with NLCs in between cell cycling. Lipids represent especially energy-demanding building blocks for the proliferating cells[55], so the possibility to incorporate NLC-derived membranes by trogocytic CLL cells could further optimize their metabolic demands.

This work underlies the central role of NLCs in supporting CLL cells, and characterizes a novel, trogocytosis-mediated type of pro-tumoral interaction between these two cell types. In summary, our work demonstrates that FOLR2 is a specific marker of protumoral NLCs, and that CLL cells engage in trogocytosis with these cells, resulting in FOLR2 acquisition. Following trogocytosis-mediated transfer of the functional FOLR2, CLL cells are found enriched in the fraction of activated and proliferating cancer cells, particularly when folic acid is scarce. In this context, trogocytosis-mediated transfer of FOLR2 represents a novel mechanism of CLL adaptation to a microenvironment with decreased access to nutrients. Trogocytosis remains an elusive phenomenon, with many challenges regarding the description of its exact extent and role in cancer progression. We believe that uncovering the intricacy of trogocytosis in CLL could increase our understanding of the cancer cell interactions within the TME, leading to more efficient therapeutic strategies, potentially relevant for other types of cancers.

Bibliography

1. Kipps TJ, Stevenson FK, Wu CJ, et al. Chronic lymphocytic leukaemia. *Nat Rev Dis Primers*. 2017;3(Cll):
2. Ponzoni M, Doglioni C, Caligaris-Cappio F. Chronic lymphocytic leukemia: The pathologist's view of lymph node microenvironment. *Semin Diagn Pathol*. 2011;28(2):161–166.
3. Lapieaux L, Delforfe A, Bron P, De Bruyn C, Slryckmans P. Chronic lymphocytic leukemia (CLL) B-lymphocytes but not normal B-lymphocytes are rescued from apoptosis by contact with bone marrow stromal cells. *Exp Hematol*. 1997;25(8):862.
4. Burger JA, Quiroga MP, Hartmann E, et al. High-level expression of the T-cell chemokines CCL3 and CCL4 by chronic lymphocytic leukemia B cells in nurselike cell cocultures and after BCR stimulation. *Blood*. 2009;113(13):3050–3058.
5. Boissard F, Laurent C, Ramsay AG, et al. Letter to the editor: Nurse-like cells impact on disease progression in chronic lymphocytic leukemia. *Blood Cancer J*. 2016;6(1):.
6. Zaaboub R, Vimeux L, Contremoulins V, et al. Nurselike cells sequester B cells in disorganized lymph nodes in chronic lymphocytic leukemia via alternative production of CCL21. *Blood Adv*. 2022;6(16):4691–4704.
7. Guo Y, Pei H, Lu B, et al. Aberrantly expressed Wnt5a in nurse-like cells drives resistance to Venetoclax in chronic lymphocytic leukemia. *Cell Death Discov*. 2022;8(1):1–9.
8. Koehrer S, Burger JA. Chronic Lymphocytic Leukemia: Disease Biology. *Acta Haematol*. 2024;147(1):9–23.
9. Burger JA, Tsukada N, Burger M, et al. Blood-derived nurse-like cells protect chronic lymphocytic leukemia B cells from spontaneous apoptosis through stromal cell-derived factor-1. *Blood*. 2000;96(8):2655–2663.
10. Tsukada N, Burger JA, Zvaifler NJ, Kipps TJ. Distinctive features of "nurselike" cells that differentiate in the context of chronic lymphocytic leukemia. *Blood*. 2002;99(3):1030–1037.
11. Ysebaert L, Fournié JJ. Genomic and phenotypic characterization of nurse-like cells that promote drug resistance in chronic lymphocytic leukemia. *Leuk Lymphoma*. 2011;52(7):1404–1406.
12. Boissard F, Fournié JJ, Laurent C, Poupot M, Ysebaert L. Nurse like cells: Chronic lymphocytic leukemia associated macrophages. *Leuk Lymphoma*. 2015;56(5):1570–1572.
13. Domagala M, Ysebaert L, Ligat L, et al. IL-10 rescues CLL survival through repolarization of inflammatory nurse-like cells. *Cancers (Basel)*. 2022;14(1):1–15.
14. Talbot H, Saada S, Barthout E, et al. BDNF belongs to the nurse-like cell secretome and supports survival of B chronic lymphocytic leukemia cells. *Sci Rep*. 2020;10(1):1–9.
15. Elisa ten Hacken 1, Maria Gounari, 2, 3 Jaap Willem Back 4, Ekaterina Shimanovskaya 4, et al. Calreticulin as a novel B-cell receptor antigen in chronic lymphocytic leukemia. *J ECT*. 2011;27(2):175–177.
16. Vaca AM, Ioannou N, Sivina M, et al. Activation and expansion of T-follicular helper cells in chronic lymphocytic leukemia nurselike cell co-cultures. *Leukemia*. 2022;36(5):1324–1335.
17. Jia L, Clear A, Liu FT, et al. Extracellular HMGB1 promotes differentiation of nurse-like cells in chronic lymphocytic leukemia. *Blood*. 2014;123(11):1709–1719.

18. Boissard F, Fournié JJ, Quillet-Mary A, Ysebaert L, Poupot M. Nurse-like cells mediate ibrutinib resistance in chronic lymphocytic leukemia patients. *Blood Cancer J*. 2015;5:e355.
19. Sanchez-Lopez E, Ghia EM, Antonucci L, et al. NF-κB-p62-NRF2 survival signaling is associated with high ROR1 expression in chronic lymphocytic leukemia. *Cell Death Differ*. 2020;27(7):2206–2216.
20. Chen Y, Chen L, Yu J, et al. Cirmtuzumab blocks Wnt5a/ROR1 stimulation of NF-kB to repress autocrine STAT3 activation in chronic lymphocytic leukemia. *Blood*. 2019;134(13):1084–1094.
21. Burger M, Hartmann T, Krome M, et al. Small peptide inhibitors of the CXCR4 chemokine receptor (CD184) antagonize the activation, migration, and antiapoptotic responses of CXCL12 in chronic lymphocytic leukemia B cells. *Blood*. 2005;106(5):1824–1830.
22. Deaglio S, Vaisitti T, Bergui L, et al. CD38 and CD100 lead a network of surface receptors relaying positive signals for B-CLL growth and survival. *Blood*. 2005;105(8):3042–3050.
23. Boissard F, Tosolini M, Ligat L, et al. Nurse-like cells promote CLL survival through LFA-3/CD2 interactions. *Oncotarget*. 2017;8(32):52225–52236.
24. Joly E, Hudrisier D. What is trogocytosis and what is its purpose? *Nat Immunol*. 2003;4(9):815.
25. Schriek P, Ching AC, Moily NS, et al. Marginal zone B cells acquire dendritic cell functions by trogocytosis. *Science (1979)*. 2022;375(6581):.
26. Shin JH, Jeong J, Maher SE, et al. Colon cancer cells acquire immune regulatory molecules from tumor-infiltrating lymphocytes by trogocytosis. *Proc Natl Acad Sci U S A*. 2021;118(48):.
27. Kawashima M, Higuchi H, Kotani A. Significance of trogocytosis and exosome-mediated transport in establishing and maintaining the tumor microenvironment in lymphoid malignancies. *Journal of Clinical and Experimental Hematopathology*. 2021;61(4):192–201.
28. Cresswell GM, Wang B, Kischuk EM, et al. Folate Receptor Beta Designates Immunosuppressive Tumor-Associated Myeloid Cells That Can Be Reprogrammed with Folate-Targeted Drugs. *Cancer Res*. 2021;81(3):671–684.
29. Xia W, Hilgenbrink AR, Matteson EL, et al. A functional folate receptor is induced during macrophage activation and can be used to target drugs to activated macrophages. *Blood*. 2009;113(2):438–446.
30. Zhang F, Huang B, Utturkar SM, et al. Tumor-specific activation of folate receptor beta enables reprogramming of immune cells in the tumor microenvironment. *Front Immunol*. 2024;15(February):1–14.
31. Rafael Samaniego 1,* , Ángeles Domínguez-Soto 2,*, Manohar Ratnam 3, Takami Matsuyama 4, Paloma Sánchez-Mateos 5, Ángel L. Corbí 2,† and Amaya Puig-Kröger 6 †. Folate Receptor β (FRβ) Expression in Tissue-Resident and Tumor-Associated Macrophages Associates with and Depends on the Expression of PU.1. 2020;1–17.
32. Samaniego R, Palacios BS, Domiguez-Soto Á, et al. Macrophage uptake and accumulation of folates are polarization-dependent in vitro and in vivo and are regulated by activin A. *J Leukoc Biol*. 2014;95(5):797–808.
33. Ducker GS, Rabinowitz JD. One-Carbon Metabolism in Health and Disease. *Cell Metab*. 2017;25(1):27–42.

34. Bied M, Ho WW, Ginhoux F, Blériot C. Roles of macrophages in tumor development: a spatiotemporal perspective. *Cell Mol Immunol*. 2023;20(9):983–992.
35. Puig-Kröger A, Sierra-Filardi E, Domínguez-Soto A, et al. Folate receptor β is expressed by tumor-associated macrophages and constitutes a marker for M2 anti-inflammatory/regulatory Macrophages. *Cancer Res*. 2009;69(24):9395–9403.
36. Rechavi O, Goldstein I, Kloog Y. Intercellular exchange of proteins: The immune cell habit of sharing. *FEBS Lett*. 2009;583(11):1792–1799.
37. De Jesus E, Keating JJ, Kularatne SA, et al. Comparison of Folate Receptor Targeted Optical Contrast Agents for Intraoperative Molecular Imaging. *Int J Mol Imaging*. 2015;2015:1–10.
38. Schleiss C, Ilias W, Tahar O, et al. BCR-associated factors driving chronic lymphocytic leukemia cells proliferation ex vivo. *Sci Rep*. 2019;9(1):1–12.
39. De Totero D, Meazza R, Capaia M, et al. The opposite effects of IL-15 and IL-21 on CLL B cells correlate with differential activation of the JAK/STAT and ERK1/2 pathways. *Blood*. 2008;111(2):517–524.
40. Gupta R, Li W, Yan XJ, et al. Mechanism for IL-15–Driven B Cell Chronic Lymphocytic Leukemia Cycling: Roles for AKT and STAT5 in Modulating Cyclin D2 and DNA Damage Response Proteins. *The Journal of Immunology*. 2019;202(10):2924–2944.
41. Ghamlouch H, Ouled-Haddou H, Damaj G, et al. A Combination of Cytokines Rescues Highly Purified Leukemic CLL B-Cells from Spontaneous Apoptosis In Vitro. *PLoS One*. 2013;8(3):1–9.
42. Bulian P, Shanafelt TD, Fegan C, et al. CD49d is the strongest flow cytometry-based predictor of overall survival in chronic lymphocytic leukemia. *Journal of Clinical Oncology*. 2014;32(9):897–904.
43. Smilevska T, Stamatopoulos K, Samara M, et al. Transferrin receptor-1 and 2 expression in chronic lymphocytic leukemia. *Leuk Res*. 2006;30(2):183–189.
44. Uxa S, Castillo-Binder P, Kohler R, et al. Ki-67 gene expression. *Cell Death Differ*. 2021;28(12):3357–3370.
45. Bechtel TJ, Reyes-Robles T, Fadeyi OO, Oslund RC. Strategies for monitoring cell–cell interactions. *Nat Chem Biol*. 2021;17(6):641–652.
46. Propper DJ, Balkwill FR. Harnessing cytokines and chemokines for cancer therapy. *Nat Rev Clin Oncol*. 2022;19(4):237–253.
47. Kalluri R, McAndrews KM. The role of extracellular vesicles in cancer. *Cell*. 2023;186(8):1610–1626.
48. Armingol E, Officer A, Harismendy O, Lewis NE. Deciphering cell–cell interactions and communication from gene expression. *Nat Rev Genet*. 2021;22(2):71–88.
49. Lu T, Ma R, Li Z, et al. Hijacking TYRO3 from tumor cells via trogocytosis enhances NK-cell effector functions and proliferation. *Cancer Immunol Res*. 2021;9(10):1229–1241.
50. Gutiérrez-Seijo A, García-Martínez E, Barrio-Alonso C, et al. Activin A Sustains the Metastatic Phenotype of Tumor-Associated Macrophages and Is a Prognostic Marker in Human Cutaneous Melanoma. *Journal of Investigative Dermatology*. 2022;142(3):653-661.e2.
51. Machacek C, Supper V, Leksa V, et al. Folate Receptor β Regulates Integrin CD11b/CD18 Adhesion of a Macrophage Subset to Collagen. *The Journal of Immunology*. 2016;197(6):2229–2238.
52. Vanherberghen B, Andersson K, Carlin LM, et al. Human and murine inhibitory natural killer cell receptors transfer from natural killer cells to target cells. 2004.

53. Ikhlef L, Ratti N, Durand S, et al. Extracellular vesicles from type-2 macrophages increase the survival of chronic lymphocytic leukemia cells ex vivo. *Cancer Gene Ther*. 2024;(November 2023):
54. Ahmed KA, Xiang J. Mechanisms of cellular communication through intercellular protein transfer. *J Cell Mol Med*. 2011;15(7):1458–1473.
55. Snaebjornsson MT, Janaki-Raman S, Schulze A. Greasing the Wheels of the Cancer Machine: The Role of Lipid Metabolism in Cancer. *Cell Metab*. 2020;31(1):62–76.

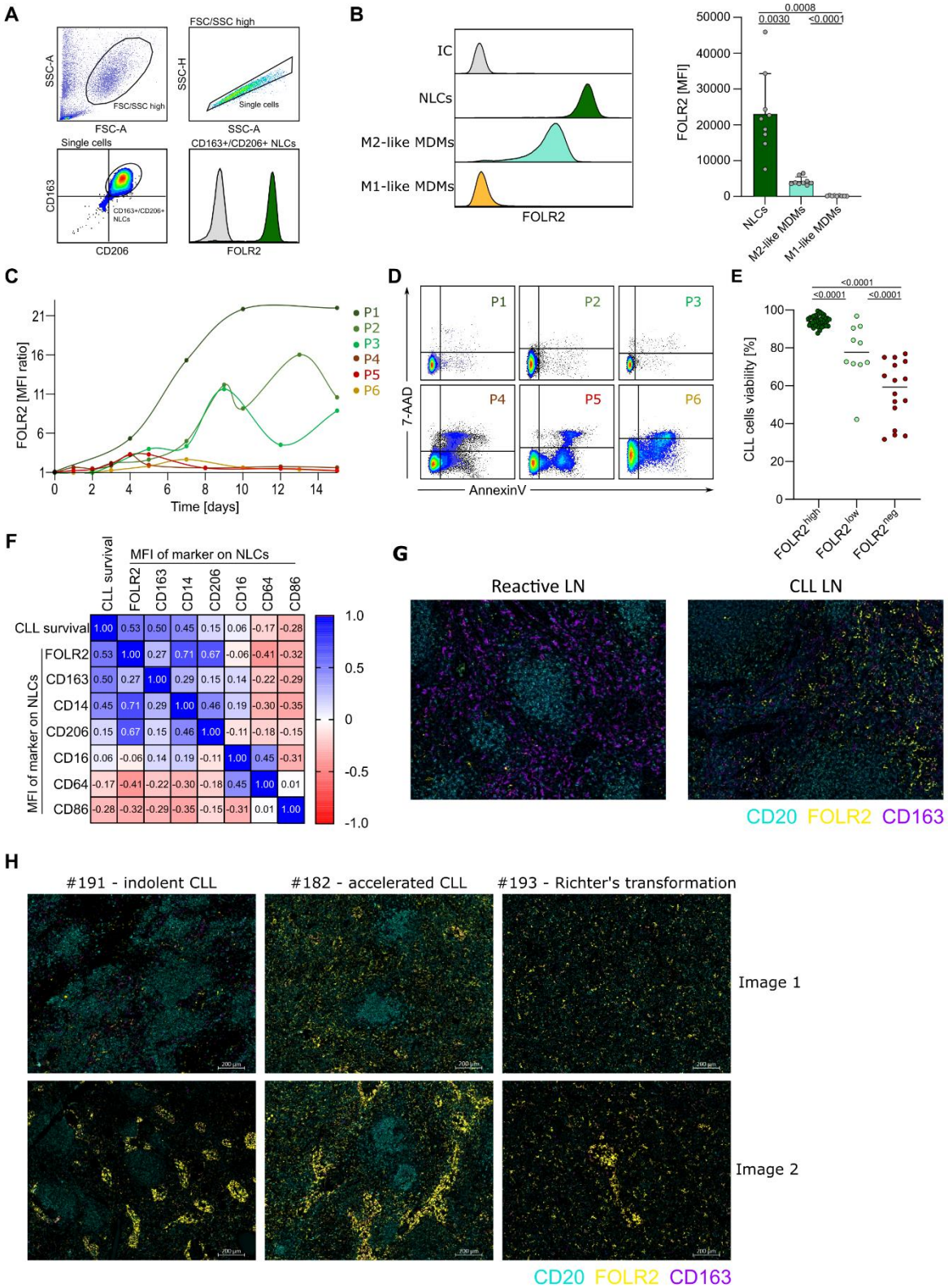

Fig.1 FOLR2 is a marker of protective NLCs. A) FC analysis of the expression of FOLR2 on a subpopulation of NLCs ($CD163^{+}CD206^{+}$) generated in a culture of PBMC from a CLL patient (grey: isotypic control; green: anti-FOLR2). **B)** Comparison of FOLR2 expression on various types of *in vitro* generated macrophages: NLCs,

M2-like and M1-like macrophages (Left: representative histograms; right: compilation of 9 independent experiments. **C)** Kinetics of FOLR2 expression during CD14$^+$ monocyte to NLC differentiation in CLL PBMC cultures for 14 days measured by FC (MFI ratio: anti-FOLR2/isotopic control). **D)** FC analysis of the CLL cells viability from CLL PBMC cultures on day 12 (annexin V/7-AAD staining). **E)** Percentage of CLL cells viability for the three groups of CLL patients according to the FOLR2 expression on NLCs. **F)** Correlation of the FOLR2 expression on NLCs with the CLL cells viability. **G)** Multiplex immunofluorescence (mIF) of a reactive lymph node and a lymph node from a CLL patient with the staining of CD20 (cyan), FOLR2 (yellow) and CD163 (purple). **H)** Representative images of lymph nodes from CLL patients, with various stages of the disease, from indolent to accelerated and Richter transformation; stained with anti-CD20 (cyan), anti-FOLR2 (yellow) and anti-CD163 (purple) antibodies (objective: x20).

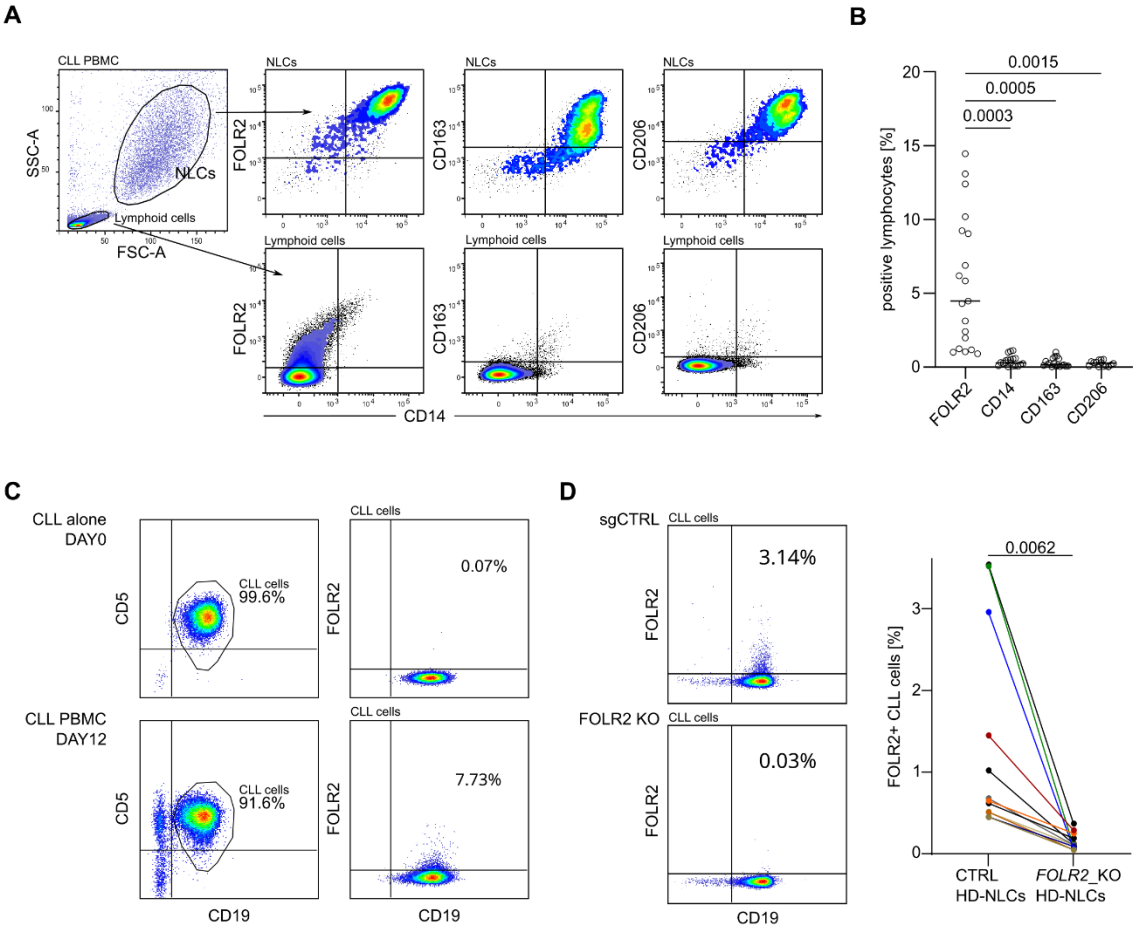

Fig.2 Detection of FOLR2 on the surface of CLL cells. A) FC analysis of the expression of FOLR2, CD14, CD163 and CD206 on cells from a culture of PBMC from a CLL patient at day 12 of *in vitro* culture, results for big, granular cells corresponding to NLCs (upper panel) and small cells corresponding to lymphoid cells (bottom panel). **B)** Expression of FOLR2, CD14, CD163, CD206 on the small cells (lymphocytes including CLL cells) of CLL PBMC cultures at day 12 (19 donors). **C)** FOLR2 expression on CLL cells (CD5$^+$CD19$^+$) alone at day 0 or in PBMC culture on day 12. **D)** left: FOLR2 expression by CLL cells in co-culture with CTRL HD-NLCs or FOLR2 KO NLCs; right: Percentage of FOLR2$^+$ CLL cells in co-cultures with CTRL HD-NLCs or *FOLR2* KO HD-NLCs (10 independent experiments).

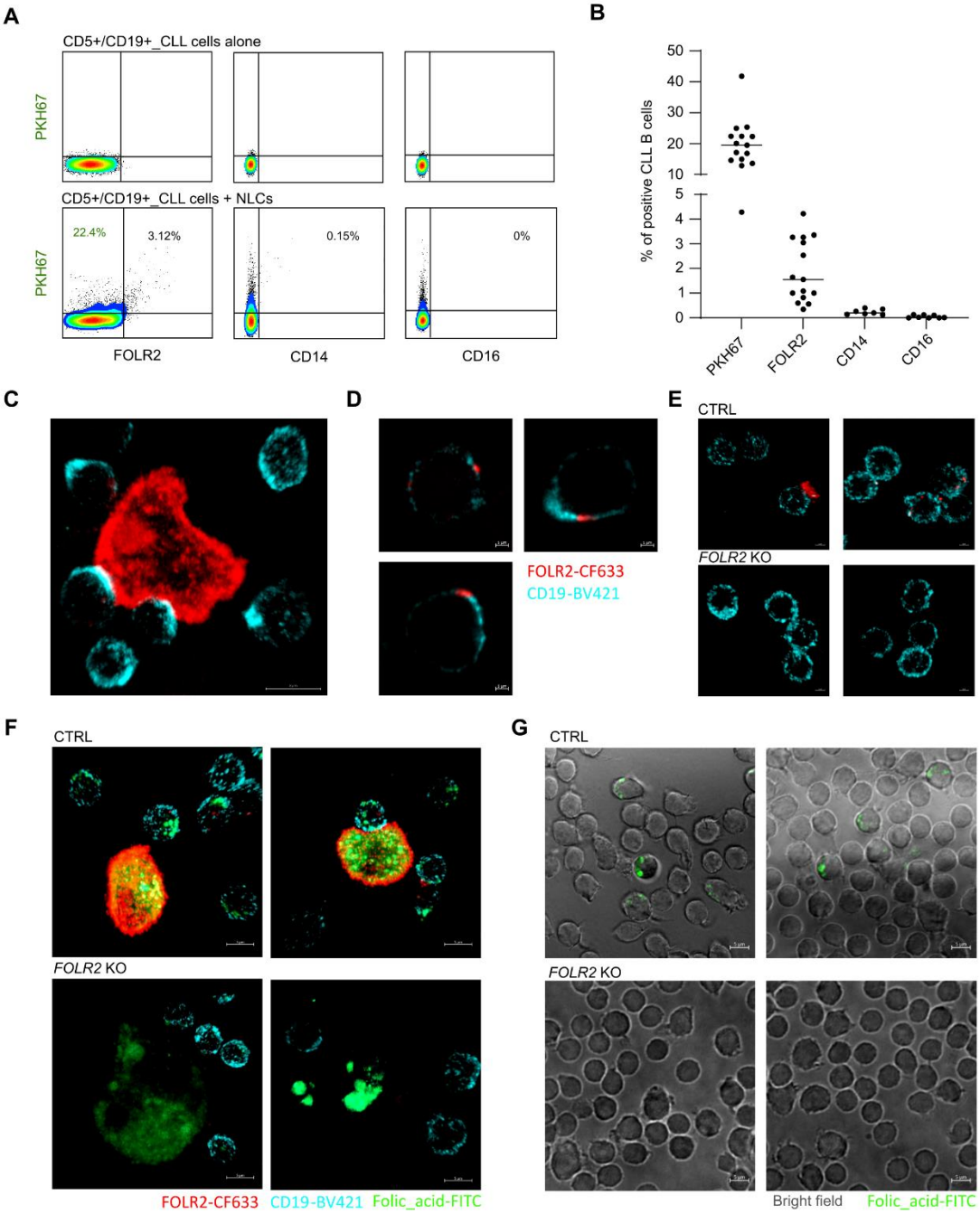

Fig.3 CLL cells acquire functional FOLR2 from NLCs by trogocytosis. A) FC analysis of the PKH67/FOLR2/CD14/CD16 signal on CLL cells after 4-hours of co-culture with PKH67^{+} NLCs (upper: CLL cells alone; below: co-culture with NLCs). **B)** Percentage of CLL cells positive for PKH67, FOLR2, CD14 and CD16 after 4-hours of co-culture with NLCs (15 independent experiments). **C-E)** Confocal microscopy (x63 magnification) of co-culture of CLL cells (CD19^{+}: cyan) and NLCs (FOLR2^{+}: red) during 4-hours showing: the contact of NLCs and CLL cells (**C**), the acquisition of FOLR2 patches by CLL cells after contact with NLCs (**D**) and the absence of detection of FOLR2 signal on CLL cells after co-culture with *FOLR2* KO HD-NLCs (**E**). **F)** Confocal microscopy of a 4-hours co-culture of CLL cells with CTRL HD-NLCs (upper) or with FOLR2 KO NLCs (below) incubated with folic acid-FITC (green) then stained with anti-FOLR2-CF633 (red) and with CD19-

BV421 (cyan). **G)** Confocal microscopy of purified CLL cells after co-culture with CTRL HD-NLCs (upper) or *FOLR2* KO HD-NLCs (below), following by incubation with folic acid-FITC for 90 min.

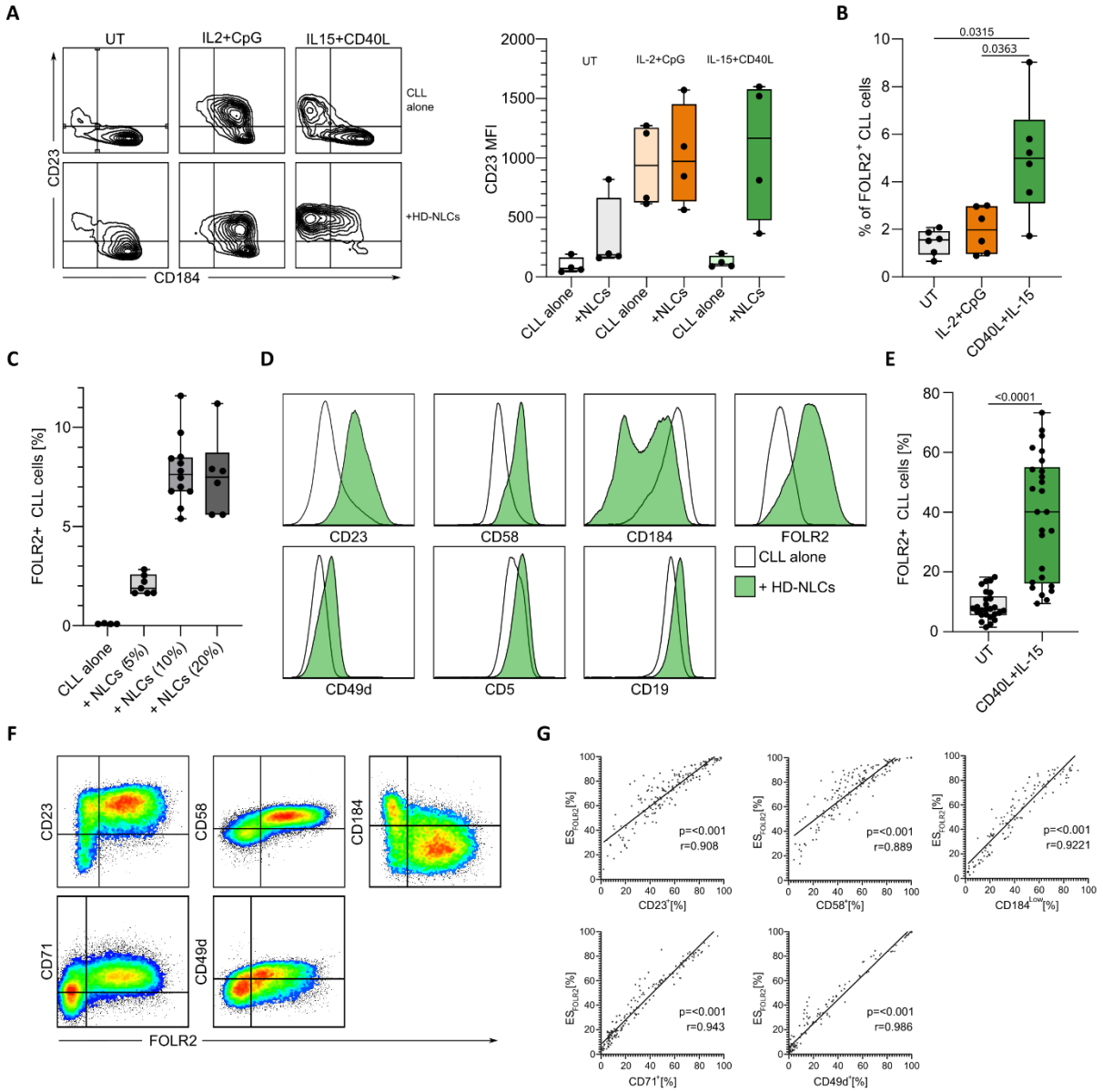

Fig.4 FOLR2 transfer is positively associated with activation of CLL cells. A) FC analysis of the CD23 and CD184 expression on CLL cells alone or in the presence of HD-NLCs incubated or not with IL-2+CpG or CD40L+IL-15 (left: one representative experiment; right: four independent experiments). **B)** Percentage of FOLR2$^+$ CLL cells analyzed by FC following co-culture with HD-NLCs in the presence or not of IL-2+CpG or CD40L+IL-15. **C)** Percentage of FOLR2$^+$ CLL cells after co-culture with increasing amount of NLCs: 5, 10 or 20%. **D)** FC analysis of expression of CD23, CD58, CD184, FOLR2, CD49d, CD5 and CD19 on CLL cells cultivated alone (white) or with HD- NLCs (green) in the presence of CD40L+IL-15. **E)** Percentage of FOLR2$^+$ CLL cells in co-culture with HD-NLCs in the presence or not of CD40L+IL-15. **F)** Expression of CD23, CD58, CD184, CD71, CD49d, and FOLR2 on CLL cells after co-culture with HD-NLCs in the presence of CD40+IL-15. **G)** Representation of the correlation between the total fraction of CLL cells positive for the different

CLL markers (CD23, CD58, CD71, CD49d and CD184) and the percentage of FOLR2^{+} cells expressing each of these markers (5 independent experiments, 12 patients, >200 samples).

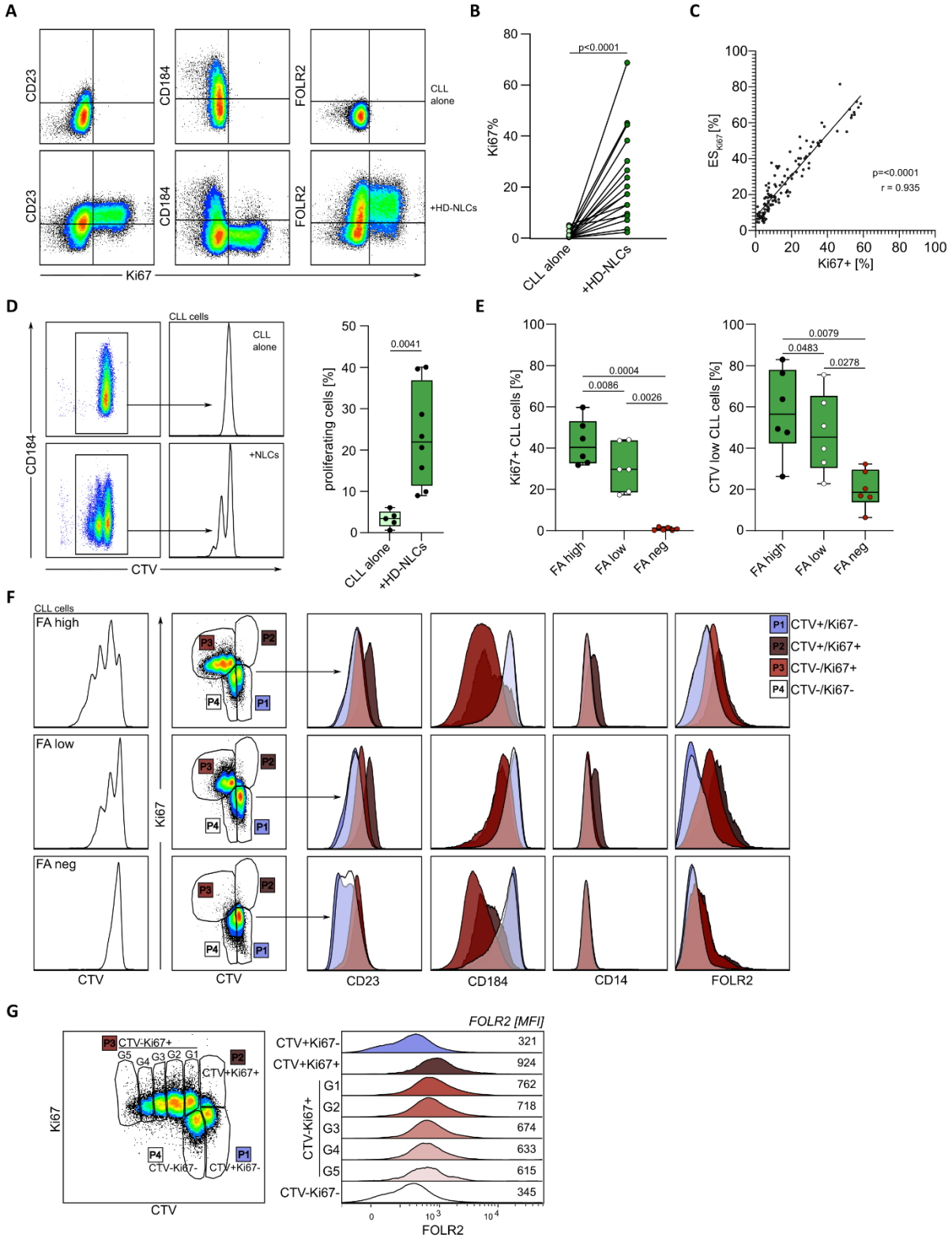

Fig.5 Trogocytic FOLR2^{+} CLL cells have an advantage in proliferation in FA deprived conditions. A) FC

analysis of expression of Ki67, CD23, CD184 and FOLR2 on CLL cells cultured alone or with HD-NLCs in the presence of CD40L+Il15. **B)** Percentage of Ki67^{+} CLL cells cultured alone or with HD-NLCs in the presence of CD40L+IL-15. **C)** Correlation between FOLR2 acquisition and Ki67 expression by CLL cells co-cultured with HD-NLCs in the presence of CD40L+IL-15 (5 independent experiments, 12 patients, >200 samples). **D)** CTV dilution assay of CLL cells cultured alone or with HD-NLCs in the presence of CD40L+IL-15: exemplary FC results (left), cumulative results from 8 patients represented as percentage of proliferating cells based on decrease in CTV signal (right). **E)** Percentage of actively cycling (Ki67^{+}, left) and total fraction of cycling (CTV low, right) CLL cells in co-culture with HD-NLCs in the presence of CD40L+IL-15, in the media with various concentrations of folic acid (FA). **F)** FC analysis of CD23, CD184, CD14 and FOLR2 signal on CLL cells stratified based on Ki67/CTV level (P1. CTV^{high}Ki67^{-}: quiescent cells that did not divide; P2. CTV^{high}Ki67^{+}: cells right before the first division; P3. CTV^{low}Ki67^{+}: actively cycling cells after previous division; P4. CTV^{low}Ki67^{-}: cells after cycling, quiescent again). **G)** FC analysis of FOLR2 level represented as MFI on CLL cells, depending on the proliferative status (Ki67/CTV) and subsequent cell generations (G1-G5).

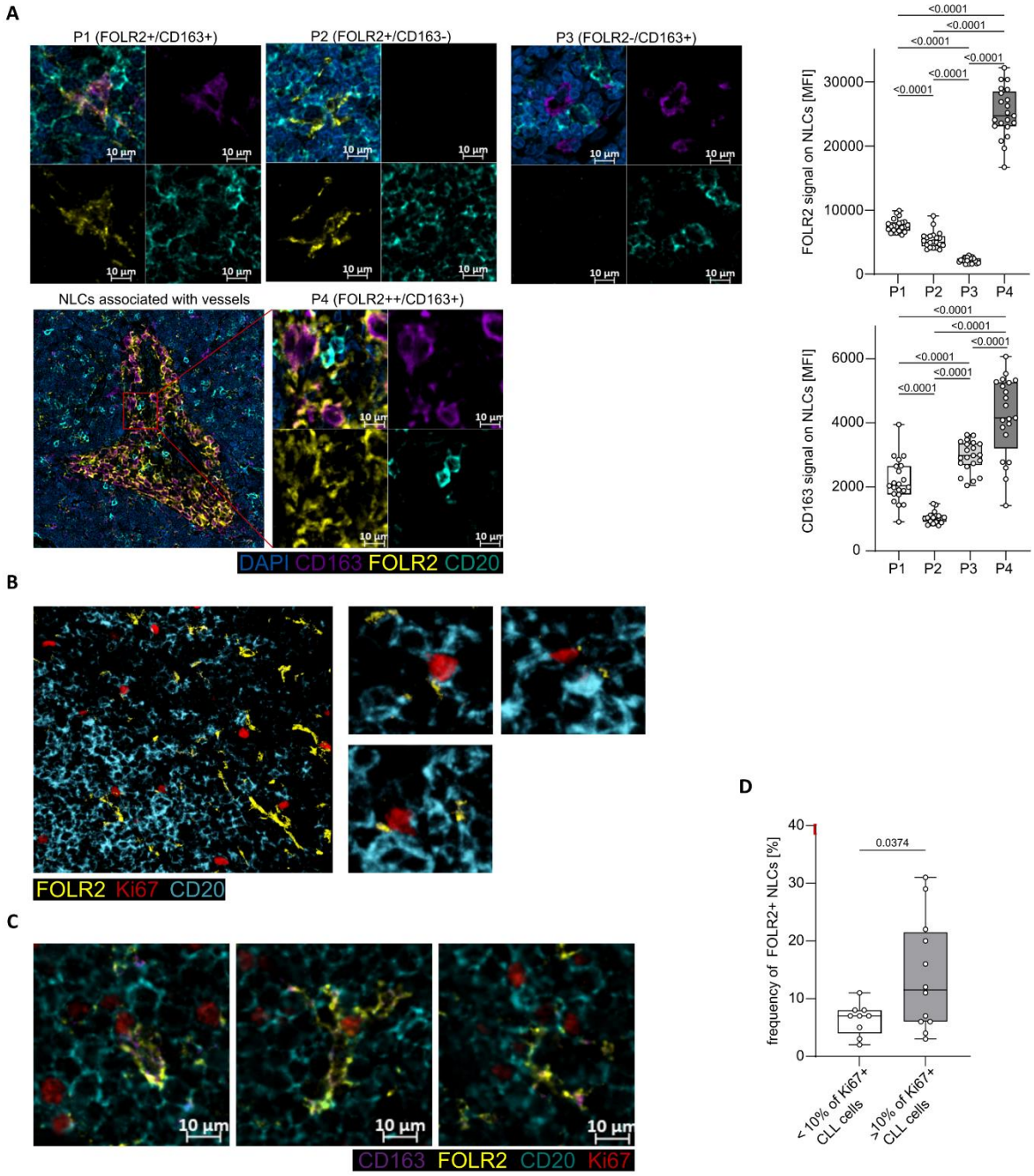

Fig. 6 Detection of FOLR2⁺ CLL cells *in vivo* and correlation between FOLR2⁺ NLCs and CLL cells proliferation.

CLL lymph node tissue sections (n=21 patients) of 4µm were stained with DAPI (blue) and anti-CD20 (cyan), anti-FOLR2 (yellow), anti-CD163 (purple), anti-Ki67 (red) antibodies, and visualized with confocal microscope (objective: x20). A) Left – representative images of 4 subgroups of NLCs, differentiated based on FOLR2 and CD163 expression: P1 ($FOLR2^{+}/CD163^{+}$), P2 ($FOLR2^{+}/CD163^{-}$), P3 ($FOLR2^{-}/CD163^{+}$), P4 ($FOLR2^{+++}CD163^{++}$) and association with vasculature (P4). Right – quantitative analysis of FOLR2 and CD163 MFI on different subgroups of NLCs. B) Detection of FOLR2 signal patches on $CD20^{+}$ CLL cells. C) $FOLR2^{+}/CD163^{+}$ NLCs are densely surrounded by $Ki67^{+}$ CLL cells. D) FOLR2+ NLCs are more frequent in the LNs where CLL cells have higher proliferative index.

	Patient	Sex	Age	Mutational status	CLL type	Richter's transformation before sampling	Reactive T cell infiltration	Binet stage before sampling	Treatment before sampling	Treatment post-sampling	Patient status
1	179	M	82	n.d.	Accelerated	Richter		A		R-miniCHOP	n.d.
2	180	F	86	n.d.	Accelerated	Richter-like	1	n.d.			0
3	181	M	74	n.d.	Accelerated	Richter-like	0	A	RCD	R-miniCHVP	1
4	182	M	69	n.d.	Accelerated	n.d.	0	n.d.	0		1
5	183	M	71	UCLL	Accelerated	n.d.	1	B	0	Ibrutinib	0
6	184	F	77	MCLL	Accelerated	n.d.	0	A	0	GA101-CLB	0
7	185	M	65	UCLL	Accelerated	0	1	B	Ibrutinib	R-VENETOCLAX	0
8	186	F	77	MCLL	Accelerated	0	1	B	0	Obituzumab+Chloraminophene	0
9	187	F	76	n.d.	Indolent	0	0	a	0	0	n.d.
10	188	M	76	n.d.	Accelerated	n.d.	0	A	Imbruvica		1
11	189	M	79	n.d.	Accelerated	n.d.	1	A	0	RCD	1
12	190	F	78	n.d.	Accelerated	0	0	B	RFC	0	0
13	191	F	72	n.d.	Indolent	0	0	n.d.	0	after Chemo	0
14	192	M	75	UCLL	Accelerated	n.d.	0	B	0	Acalabrutinib	0
15	193	M	83	n.d.	Accelerated	Richter	0	n.d.	Imbruvica		0
16	194	F	85	UCLL	Accelerated	0	1	C	R-Bendamustine	Acalabrutinib	0
17	195	M	65	UCLL	Accelerated	Richter	1	A	0	R-CHOP	0
18	196	M	82	MCLL	Accelerated	n.d.	1	A	0	0	0
19	197	F	74	n.d.	Indolent	0	0	n.d.	n.d.	n.d.	n.d.
20	198	M	61	n.d.	n.d.	n.d.	0	n.d.	n.d.	n.d.	n.d.
21	199	M	1317 4	n.d.	n.d.	n.d.	1	n.d.	n.d.	n.d.	n.d.
22	200	F	74	MCLL	Accelerated	n.d.	0	C	FCR	R-Venetoclax	0
23	201	M		n.d.	Indolent		0	n.d.	n.d.	n.d.	0
24	202	F	83	UCLL	n.d.		0	n.d.	n.d.	n.d.	0
25	203	F	81	n.d.	Indolent		0	n.d.	n.d.	n.d.	0